



Induction of 2D grid structure from amphiphilic pyrene assembly by charge transfer interaction

Bowen Shen^a, Il-Soo Park^b, Yongju Kim^c, Huaxin Wang^a, Myongsoo Lee^{a,*}

^a Department of Chemistry, Fudan University, Shanghai 200438, China

^b Department of Chemistry, Seoul National University, Seoul 08826, Korea

^c KU-KIST Graduate School of Converging Science and Technology, Korea University, Seoul 02841, Korea

Keywords: Self-assembly, Pyrene amphiphile, Charge-transfer, Nanofiber, 2d grids, Crystallization

In this work, we report the spontaneous formation of 2-dimensional (2D) grid structures through charge transfer interactions of pyrene amphiphiles. Pure pyrene amphiphiles self-assemble into long nanofibers in aqueous solution. Remarkably, these aqueous nanofibers transform into a 2D grid structure upon charge transfer complexation. The charge transfer interaction induces crystallization of the aromatic core part, leading to discrete micelles with up and down hydrophilic chains, and hydrophobic side faces. Eventually, the anisotropic micelles grow in a 2-dimensional way through side-by-side interactions to form unusual 2D grid structures.

1 Introduction

The development of novel nanostructures by self-assembly of amphiphilic block molecules has received a great attention because of their potential in biomaterials and nanotechnology [1–5]. The careful design of the molecular shape and the control of relative volume fraction between hydrophilic and hydrophobic segments in block molecules can give rise to a variety of the well-defined supramolecular structures [6–10]. Especially, in the case of rigid-flexible block molecules, the large difference in their stiffness between the rigid hydrophobic segments and the flexible hydrophilic coil segments leads to a variety of morphologies such as spheres, cylinders, ribbons, vesicles, toroids, tubes, scrolls in aqueous solutions [11–29]. Although many studies have been done in well-defined nanostructures using rigid-flexible block molecules, it has a limitation on the diversity because most of the self-assembled nanostructures are formed from unimolecular

assembly. The repertoire of supramolecular assembly can be significantly enhanced, if the organized structures are able to be manipulated by additional secondary interactions, such as hydrogen bonding, electrostatic interactions, and charge transfer interactions, because these secondary interactions allow the hierarchical assembly of organized structures.

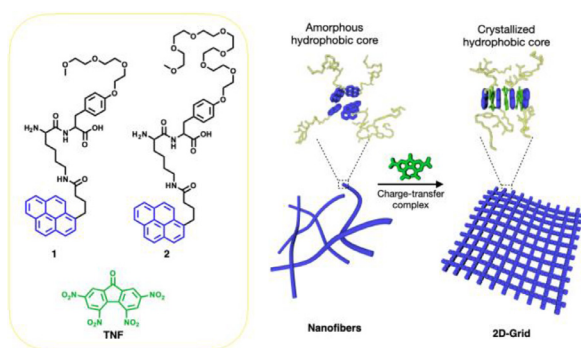
We have also demonstrated that the self-assembly of tripeptides into 0-D vesicles, 1-D twisted ribbon and 1-D flat ribbon structures could be controlled via the combination of hydrogen bonding and hydrophobic π - π interactions [30]. The primary driving force for the 1-D ribbon structure was proposed to be the directional ordering of the hydrogen bonding which is stabilized by intermolecular π - π interaction between the fluorenyl groups of neighboring antiparallel β -sheets. These results imply that a delicate balance between secondary interactions plays a critical role in the self-assembly of block amphiphiles and this can provide the opportunity to extend their scope toward construction of complex nanostructures.

We present here the formation of nanogrids from the aqueous self-assembly of amphiphilic block molecules, which is driven

* Corresponding author.

E-mail address: mslee@fudan.edu.cn (M. Lee).

Received 10 December 2020; Received in revised form 30 December 2020; Accepted 30 December 2020

**Fig. 1**

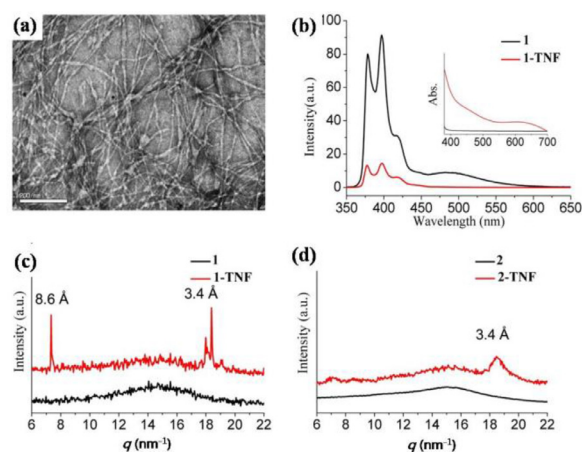
Pyrene-containing molecular structures of **1**, **2**, and structure of TNF. While pyrene amphiphiles self-assemble into the 1D nanofiber with amorphous aromatic core, pyrene-containing molecules **1** self-assemble into the 2D nanogrid structure through aromatic core crystallization by charge-transfer complexation with TNF.

by pseudo-crystallization of hydrophobic core through the combination of the secondary forces such as hydrophobic π - π interactions, ionic repulsions, and charge transfer interactions (Fig. 1).

Most of self-assembly systems using rigid-flexible block molecules consist of amorphous hydrophobic cores because the intermolecular π - π interactions are relatively weak in solution. We anticipate that strong intermolecular interactions in the core will induce the crystallization of the aromatic segments to create a unique nanostructure which is unable to observe in conventional rigid-flexible molecules. With this idea in mind, we have performed charge transfer complexation in the aromatic core to enhance intermolecular interactions and investigated the nanostructures in the aqueous solution. For this purpose, we prepared dipeptides which have a lysine functionalized with pyrene as an electron rich hydrophobic segment at its ϵ -position and a tyrosine modified with an oligoethylene glycol as a hydrophilic unit (Fig. 1). For charge transfer interactions, 2, 4, 5, 7-tetranitrofluorenone (TNF) was used as a hydrophobic guest molecule and an electron deficient acceptor for the charge transfer complex.

2 Results and discussion

We first investigated the self-assembly behavior of pyrene-based amphiphiles, **1** and **2**, in aqueous solutions. Transmission electron microscopy (TEM) studies showed that both molecules self-assemble into stable 1D nanofibers with about 8 nm in diameter and micrometer-scale in the length (Fig. 2a and Figure S2a). The individual nanofiber showed elongated fibrillar structures through further assembly. The fluorescence data of **1** and **2** in aqueous solution showed a weak excimer peak at longer wavelength regions together with high monomeric emission, which is an indication of weak inter-pyrene electronic communication because of loosely packed pyrene units in the core (Fig. 2b and S2c) [31–35]. Indeed, wide-angle X-ray scattering (WAXS) of the freeze-dried samples of **1** and **2** showed only broad halos (black line in Figs. 2c and 2d), indicating that the core parts are amorphous. Taken all data together, we concluded that the nanofibers consist

**Fig. 2**

(a) A negatively stained TEM image of **1** in water (100 μ M, scale bar: 200 nm). (b) UV-Vis absorption (inset) and fluorescence spectra ($\lambda_{\text{ex}} = 340$ nm) of **1** and **1**-TNF aqueous solutions (100 μ M). (c), (d) Wide angle X-ray scattering data of **1** and **1**-TNF, **2** and **2**-TNF, respectively.

of an amorphous hydrophobic core of pyrene units surrounded by hydrophilic oligoethylene glycol chains (Fig. 1).

To develop a novel strategy for creating complex nanostructures by fine-controlling intermolecular interactions, we hypothesized that complexation between electron rich pyrene and electron poor TNF would enhance the intermolecular interactions which drive the core parts to be crystallized [36,37]. For the investigation of crystallization effect, the complexation between pyrene containing molecules, **1** or **2**, and TNF was carried out by dissolving two molecules with a molar ratio of 1:1 in chloroform which is a good solvent for both donor and acceptor molecules. After evaporation of the organic solvent under reduced pressure, the complexes were dissolved in water. The transparent solutions turned into green color and no precipitation was observed for several months. It should be noted that TNF itself is not soluble in water due to its high hydrophobicity and the aqueous solution of the pyrene containing molecules are colorless (Figure S3). Therefore, the color appearance and solubilization of TNF in water could be attributed to the formation of charge transfer complexes between pyrene and TNF units. As shown in inset of Fig. 2b, the complex of **1** exhibits a broad absorption between 500 nm and 700 nm, which is corresponding to the characteristic absorption of the charge transfer complex. And the emission of the complex is significantly quenched compared to that of pure **1** and the excimer peak was disappeared, indicating that the quenching process occurred due to charge transfer from pyrene segments to TNF (Fig. 2b) [38–40].

To corroborate the structural changes triggered by complexation, TEM study was carried out. The negatively stained sample with uranyl acetate clearly showed that 0.01 wt% aqueous solution of **1**-TNF has a single layer of planar nets over several micrometer scales (Fig. 3a). The planar nets consist of in-plane nanopores with a square shape which has an average side of ~ 7 nm and a uniform wall cross-section of 7 nm. The formation of square grids was further confirmed by atomic force microscopic (AFM) images which shows a 2-D grid structure

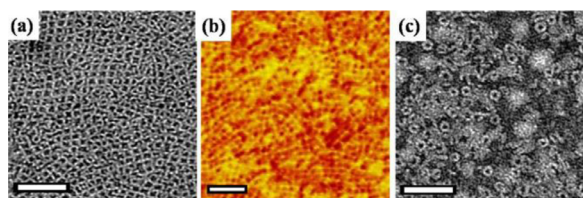


Fig. 3

(a) A negatively stained TEM image (scale bar: 100 nm) and (b) AFM image of **1-TNF** (scale bar: 100 nm) and (c) a negatively stained TEM image of **2-TNF** aqueous solutions (100 μ M, scale bar: 100 nm).

with average height of 4 nm (Fig. 3b). For direct imaging of the 2D objects formed in bulk solution, cryogenic TEM (cryo-TEM) experiments were performed with a 0.01 wt% aqueous solution. Indeed, cryo-TEM images show that the 2-D objects are consisted of in-plane square nanopore, demonstrating that the 2D grid structures form in bulk solution, not on the substrates during drying process (Figure S4). The formation of 2-D objects of **1-TNF** in bulk solution was also confirmed by fluorescence microscopy which revealed the existence of planar sheets (Figure S5). In contrast, **2-TNF** showed small toroidal rings with a uniform cross-section of 7 nm and the ring size in diameter of 20 nm (Fig. 3c).

To gain insight into the formation of the 2D grid structure, we investigated assembling behavior of the charge transfer complexes with different molar ratio between **1** and TNF. Interestingly, DLS showed the decrease in size when increasing the ratio of TNF (Figure S6a). The addition of 0.2 eq. TNF into **1** showed bimodal distribution with a major peak of about 150 nm and a minor peak about 40 nm. Increasing amount of TNF up to 0.5 eq. gives rise to decreasing the size with a major peak 30 nm and a minor peak 100 nm. TEM images revealed that the long fibers of **1** were shortened by addition of TNF (Figure S6b-c). There are two possible mechanisms for this transformation. The first is that the guest molecules could interfere the packing of rigid core segment, which induces shortening the length of 1D nanofiber [41]. The second is that the guest molecules make the strong interaction in the core to pack each other, which induces increment of steric crowding in hydrophilic parts [42]. To reduce the steric congestion, the long fibers would break-up into short fibers which allow more volume for the hydrophilic chains. To confirm this, we performed the control experiments with Nile red as a hydrophobic guest instead of TNF. We hypothesized that the intercalation of Nile red molecules will result in the break-up the long fiber to short fiber if the first assumption is reasonable. We found that, after addition of Nile red, the length of the fibers remains unchanged (Figure S7). This indicates that the second hypothesis seems to be more likely rather than the first. The charge transfer complexation between pyrene and TNF would result in close-packing between the aromatic segments. This gives rise to increasing steric repulsions between hydrophilic oligoethylene glycol chains including charge repulsion of amine groups, which prevents 1D growth of the fiber. This means that fine balance between attractive force, the charge transfer complexation, and repulsive force, the ionic and steric repulsion, plays a critical role in structural changes.

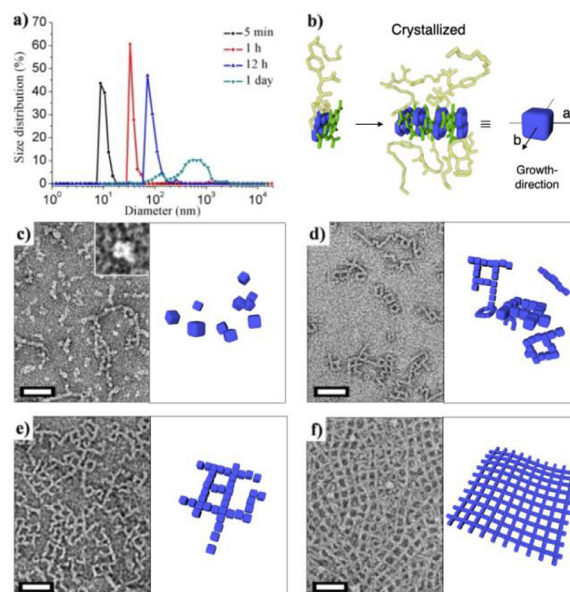


Fig. 4

(a) Size distribution of **1-TNF** aqueous solutions with increasing time. (b) Schematic representation of formation of square-shape micelle from **1-TNF** complexation. Negatively stained TEM images of **1-TNF** aqueous solutions with different time stage, (c) 5 min (d) 1 hour, (e) 12 h, and (f) 24 h (100 μ M, scale bar: 25 nm).

To estimate the packing arrangements of the aromatic cores of the complexes, wide angle X-ray scattering (WAXS) experiments were performed with freeze-dried samples. While molecule **1** was not observed any meaningful peaks, **1-TNF** sample showed sharp several peaks with 8.6 Å, 3.5 Å, and 3.4 Å distances (Fig. 2c). Based on the molecular length calculated in modeling, the first peak is corresponding to lateral distance of molecules and remaining two peaks are related with charge complex distance between **1** and TNF. In contrast, WAXS of **2-TNF** revealed only a broad and weak reflection in similar q -values, indicative of lack of the crystallinity (Fig. 2d). Based on these results, we could estimate the formation of nanogrid vs nanoring. Molecule **2** has a longer hydrophilic ethylene glycol chains than molecule **1**. The complexation of between pyrene and TNF with planar shapes in **1-TNF** gives rise to enhance the intermolecular interactions to crystallize core segments resulting in the formation of directional assemblies, angular objects, square porous sheets. Indeed, the charge transfer complexes are reported to induce a directional assembly through face-to-face packing arrangements of the two aromatic rings [43–46]. However, the core of **2-TNF** could not be highly crystallized due to the steric hindrance of adjunct larger hydrophilic volume, which might be responsible for the formation of curved-objects, rings.

In an attempt to further understand the mechanism of 2D grid formation, DLS experiments were performed at different time stages after complexation. DLS of **1-TNF** showed small sizes with unimodal distribution of 10 nm in diameter at an initial stage, which increases with time interval (Fig. 4a). This indicates that the small aggregates are initially formed via the complexation, which further merge together to form larger objects. To get

further insight of this growth mechanism, we observed the aggregation behavior by TEM experiments at different stages of structural rearrangements. At the initial state, TEM showed micelle-like objects of 10 nm sizes, with short cylindrical micelles (Fig. 4c). Interestingly, the shape of the micelle is not spherical but seems to be more angular micelles (inset of Fig. 4c). As increasing the incubation time of the solutions, TEM showed square torus structures with 90°-bent cylindrical micelles (Fig. 4d). Eventually, these micelles were observed to interconnect gradually with each other to form 2D grids on the time scale of a day, demonstrating that the grid structures are stable objects (Fig. 4e-f). These results suggest that, at the initial stage, the complexes aggregate into angular micelles with hydrophobic side faces (Fig. 4b). Subsequently, the angular micelles coalesce into a square torus structure through side-by-side hydrophobic interactions to reduce the contact between hydrophobic segments and water molecules. Eventually, the square torus structures further assemble in a lateral way to form 2D porous sheets with square pores. In contrast, **2**-TNF showed curved cylindrical micelles at an initial stage and subsequently both end of curved micelles are connected to form toroidal rings in TEM, indicating that torus ring structure is thermodynamic stable structure (Figure S8). The nanoring structure of **2**-TNF is consistent self-assembling behavior with our previous observation in rod-coil system which has amorphous hydrophobic rod aggregates [47–50]. Taken together with WAXS data, these results indicate that the crystallization of the core which is induced by pyrene-TNF charge complexation plays a pivotal role in the formation of angular micelles and their hierarchically assembled into the grid structure.

The angular micelle formation which is driven from the hydrophobic crystallization is responsible for the growth of 2D nanogrid sheets (Fig. 4b). One can raise a question why it forms porous sheet, not 2D planar sheets by the core crystallization. We hypothesized that the amine moieties in the molecular backbone prevent to grow infinite 2D planar sheet by repulsive interactions. To test this, we investigated pH-dependent self-assembly behavior of **1**-TNF. At pH 11, indeed, **1**-TNF showed planar sheet structures, demonstrating that the removal of repulsive interactions between the molecules gives rise to infinite 2D growth of the complex (Figure S9). This means that the balance of the attractive and repulsive interactions between adjunct molecules plays an important role in the formation of discrete angular micelles and subsequent nanogrid structures.

3 Conclusion

The notable feature of the pyrene amphiphiles investigated herein is their ability to self-assemble into a nanogrid 2D structure triggered by the core crystallization. The 1D fiber structures composed by amorphous hydrophobic core transform into the unique nanostructures by increasing the intermolecular interaction in hydrophobic segments via charge transfer complexation. The charge complexation of the pyrene amphiphile with a long hydrophilic chain leads to the nanoring structure, while that of the pyrene amphiphile with a short hydrophobic chain induces 2D nanogrid structures which is one of the extraordinary structures in self-assembly system [51–53]. This unique self-assembling behavior is likely to originate

form side by side connections of discrete angular micelles through the combination of the secondary forces including hydrophobic π - π interactions, ionic repulsions, and charge transfer interactions. Consequently, the enhanced attractive forces within the hydrophobic cores in the complexes would give rise to the formation of stable square torus and subsequent 2D growing into a nanogrid structure. Considering that the supramolecular self-assembly has dynamic, multicomponent nature, our approach of controlling self-assembled nanostructure using the combination of the secondary forces would allow us to develop a variety of complex nanostructures.

Declaration of Competing Interest

The authors declare that they have no known competing financial interests or personal relationships that could have appeared to influence the work reported in this paper.

Acknowledgment

This work was supported by the National Natural Science Foundation of China (21634005 and 21971084), Fudan Research Fund and Project funded by China Postdoctoral Science Foundation.

Supplementary materials

Supplementary material associated with this article can be found, in the online version, at doi:10.1016/j.giant.2021.100045.

References

- [1] T. Aida, E.W. Meijer, S.I. Stupp, Functional supramolecular polymers, *Science* 335 (2012) 813–817, doi:10.1126/science.1205962.
- [2] T. Shimizu, M. Masuda, H. Minamikawa, Supramolecular nanotube architectures based on amphiphilic molecules, *Chem. Rev.* 105 (2005) 1401–1444, doi:10.1021/cr030072j.
- [3] I. Cherny, E. Gazit, Amyloids: not only pathological agents but also ordered nanomaterials, *Angew. Chem. Int. Ed.* 47 (2008) 4062–4069, doi:10.1002/anie.200703133.
- [4] Q. Wang, J.L. Mynar, M. Yoshida, E. Lee, M. Lee, K. Okuro, K. Kinbara, T. Aida, High-water-content mouldable hydrogels by mixing clay and a dendritic molecular binder, *Nature* 463 (2010) 339–343, doi:10.1038/nature08693.
- [5] R. Ideta, F. Tasaka, W.-D. Jang, N. Nishiyama, G.-D. Zhang, A. Harada, Y. Yanagi, Y. Tamaki, T. Aida, K. Kataoka, Nanotechnology-based photodynamic therapy for neovascular disease using a supramolecular nanocarrier loaded with a dendritic photosensitizer, *Nano Lett.* 5 (2005) 2426–2431, doi:10.1021/nl051679d.
- [6] Y. Yamamoto, T. Fukushima, Y. Suna, N. Ishii, A. Saeki, S. Seki, S. Tagawa, M. Taniguchi, T. Kawai, T. Aida, Photoconductive coaxial nanotubes of molecularly connected electron donor and acceptor layers, *Science* 314 (2006) 1761–1764, doi:10.1126/science.1134441.
- [7] X. Zhang, Z. Chen, F. Würthner, Morphology control of fluorescent nanoaggregates by co-self-assembly of wedge- and dumbbell-shaped amphiphilic perylene bisimides, *J. Am. Chem. Soc.* 129 (2007) 4886–4887, doi:10.1021/ja070994u.
- [8] J. A. A. W. Elemans, R. van Hameren, R. J. M. Nolte, A. E. Rowan, Molecular materials by self-assembly of porphyrins, phthalocyanines, and perylenes, *Adv. Mater.* 18 (2006) 1251–1266, doi:10.1002/adma.200502498.
- [9] B.M. Rosen, M. Peterca, C. Huang, X. Zeng, G. Ungar, V. Percec, Deconstruction as a strategy for the design of libraries of self-assembling dendrons, *Angew. Chem. Int. Ed.* 49 (2010) 7002–7005, doi:10.1002/anie.201002514.
- [10] B.M. Rosen, C.J. Wilson, D.A. Wilson, M. Peterca, M.R. Imam, V. Percec, Dendron-mediated self-assembly, disassembly, and self-organization of complex systems, *Chem. Rev.* 109 (2009) 6275–6540, doi:10.1021/cr900157q.
- [11] E. Yashima, K. Maeda, H. Iida, Y. Furusho, K. Nagai, Helical polymers: synthesis, structures, and functions, *Chem. Rev.* 109 (2009) 6102–6211, doi:10.1021/cr900162q.
- [12] H.-J. Kim, T. Kim, M. Lee, Responsive nanostructures from aqueous assembly of rigid-flexible block molecules, *Acc. Chem. Res.* 44 (2011) 72–82, doi:10.1021/ar100111n.
- [13] B. Sun, Y. Kim, Y. Wang, H. Wang, J. Kim, X. Liu, M. Lee, Homochiral porous nanosheets for enantiomer sieving, *Nat. Mater.* 17 (2018) 599–604, doi:10.1038/s41563-018-0107-4.

- [14] H. Goto, Y. Furusho, K. Miwa, E. Yashima, Double helix formation of oligoresorcinols in water: thermodynamic and kinetic aspects, *J. Am. Chem. Soc.* 131 (2009) 4710–4719, doi:10.1021/ja808585y.
- [15] H. Shao, M. Gao, S.H. Kim, C.P. Jaroniec, J.R. Parquette, Aqueous self-assembly of L-lysine-based amphiphiles into 1D n-type nanotubes, *Chem. Eur. J.* 17 (2011) 12882–12885, doi:10.1002/chem.201102616.
- [16] M. Reches, E. Gazit, Formation of closed-cage nanostructures by self-assembly of aromatic dipeptides, *Nano Lett* 4 (2004) 581–585, doi:10.1021/nl035159z.
- [17] S. Yagai, S. Mahesh, Y. Kikkawa, K. Unoike, T. Karatsu, A. Kitamura, A. Ajayaghosh, Toroidal nanoobjects from rosette assemblies of melamine-linked oligo(p-phenyleneethynylene)s and cyanurates, *Angew. Chem. Int. Ed.* 47 (2008) 4691–4694, doi:10.1002/anie.200800417.
- [18] S. Yagai, Y. Goto, X. Lin, T. Karatsu, A. Kitamura, D. Kuzuhara, H. Yamada, Y. Kikkawa, A. Saeki, S. Seki, Self-organization of hydrogen-bonding naphthalene chromophores into J-type nanorings and H-type nanorods: impact of regioisomerism, *Angew. Chem. Int. Ed.* 51 (2012) 6643–6647, doi:10.1002/anie.201201436.
- [19] J.-K. Kim, E. Lee, M.-C. Kim, E. Sim, M. Lee, Reversible transformation of helical coils and straight rods in cylindrical assembly of elliptical macrocycles, *J. Am. Chem. Soc.* 131 (2009) 17768–17770, doi:10.1021/ja907462h.
- [20] E. Lee, J.-K. Kim, M. Lee, Reversible scrolling of two-dimensional sheets from the self-assembly of laterally grafted amphiphilic rods, *Angew. Chem. Int. Ed.* 48 (2009) 3657–3660, doi:10.1002/anie.200900079.
- [21] E. Lee, J.-K. Kim, M. Lee, Tubular stacking of water-soluble toroids triggered by guest encapsulation, *J. Am. Chem. Soc.* 131 (2009) 18242–18243, doi:10.1021/ja909279b.
- [22] J.-K. Kim, E. Lee, Y.-H. Jeong, J.-K. Lee, W.-C. Zin, M. Lee, Two-dimensional assembly of rod amphiphiles into planar networks, *J. Am. Chem. Soc.* 129 (2007) 6082–6083, doi:10.1021/ja071394y.
- [23] S. Shin, S. Lim, Y. Kim, T. Kim, T.-L. Choi, M. Lee, Supramolecular switching between flat sheets and helical tubules triggered by coordination interaction, *J. Am. Chem. Soc.* 135 (2013) 2156–2159, doi:10.1021/ja400160j.
- [24] Y. Kim, S. Shin, T. Kim, D. Lee, C. Seok, M. Lee, Switchable nanoporous sheets by the aqueous self-assembly of aromatic macrobicycles, *Angew. Chem. Int. Ed.* 52 (2013) 6426–6429, doi:10.1002/anie.201210373.
- [25] Y. Wang, Z. Huang, Y. Kim, Y. He, M. Lee, Guest-driven inflation of self-assembled nanofibers through hollow channel formation, *J. Am. Chem. Soc.* 136 (2014) 16152–16155, doi:10.1021/ja510182x.
- [26] B. Shen, Y. He, Y. Kim, Y. Wang, M. Lee, Spontaneous capture of carbohydrate guests through folding and zipping of self-assembled ribbons, *Angew. Chem. Int. Ed.* 55 (2016) 2382–2386, doi:10.1002/anie.201509190.
- [27] Y. Wang, Y. Kim, M. Lee, Static and dynamic nanosheets from selective assembly of geometric macrocycle isomers, *Angew. Chem. Int. Ed.* 55 (2016) 13122–13126, doi:10.1002/anie.201607143.
- [28] X. Liu, X. Zhou, B. Shen, Y. Kim, H. Wang, W. Pan, J. Kim, M. Lee, Porous nanosheet assembly for macrocyclization and self-release, *J. Am. Chem. Soc.* 142 (2020) 1904–1910, doi:10.1021/jacs.9b11004.
- [29] X. Feng, B. Shen, B. Sun, J. Kim, X. Liu, M. Lee, Single-layered chiral nanosheets with dual chiral void spaces for highly efficient enantiomer absorption, *Angew. Chem. Int. Ed.* 59 (2020) 11355–11359, doi:10.1002/anie.202003807.
- [30] I. Choi, I.-S. Park, J.-H. Ryu, M. Lee, Control of peptide assembly through directional interactions, *Chem. Commun.* 48 (2012) 8481–8483, doi:10.1039/C2CC31872E.
- [31] J.B. Gilroy, T. Gädt, G.R. Whittell, L. Chabanne, J.M. Mitchels, R.M. Richardson, M.A. Winnik, I. Manners, Monodisperse cylindrical micelles by crystallization-driven living self-assembly, *Nat. Chem.* 2 (2010) 566–570, doi:10.1038/nchem.664.
- [32] J.-F. Gohy, B.G.G. Lohmeijer, A. Alexeev, X.-S. Wang, I. Manners, M.A. Winnik, U.S. Schubert, Cylindrical micelles from the aqueous self-assembly of an amphiphilic poly(ethylene oxide)-b-poly(ferrocenylsilane) (PEO-b-PFS) block copolymer with a metallo-supramolecular linker at the block junction, *Chem. Eur. J.* 10 (2004) 4315–4323, doi:10.1002/chem.200400222.
- [33] M.O. Guler, R.C. Claussen, S.I. Stupp, Encapsulation of pyrene within self-assembled peptide amphiphile nanofibers, *J. Mater. Chem.* 15 (2005) 4507–4512, doi:10.1039/B509246A.
- [34] X. Zhang, S. Rehm, M.M. Safont-Sempere, F. Würthner, Vesicular perylene dye nanocapsules as supramolecular fluorescent pH sensor systems, *Nat. Chem.* 1 (2009) 623–629, doi:10.1038/nchem.368.
- [35] P. Chandar, P. Somasundaran, N.J. Turro, K.C. Waterman, Excimer fluorescence determination of solid-liquid interfacial pyrene-labeled poly(acrylic acid) conformations, *Langmuir* 3 (1987) 298–300, doi:10.1021/la00074a026.
- [36] V. Percec, M. Glodde, T.K. Bera, Y. Miura, I. Shiyonovskaya, K.D. Singer, V.S.K. Balagurusamy, P.A. Heiney, I. Schnell, A. Rapp, H.-W. Spiess, S.D. Hudson, H. Duan, Self-organization of supramolecular helical dendrimers into complex electronic materials, *Nature* 419 (2002) 384–387, doi:10.1038/nature01072.
- [37] W. Pisula, M. Kastler, D. Wasserfallen, J.W.F. Robertson, F. Nolde, C. Kohl, K. Müllen, Pronounced supramolecular order in discotic donor-acceptor mixtures, *Angew. Chem. Int. Ed.* 45 (2006) 819–823, doi:10.1002/anie.200500669.
- [38] K. Liu, C. Wang, Z. Li, X. Zhang, Superamphiphiles based on directional charge-transfer interactions: from supramolecular engineering to well-defined nanostructures, *Angew. Chem. Int. Ed.* 50 (2011) 4952–4956, doi:10.1002/anie.201007167.
- [39] V.J. Bradford, B.L. Iverson, Amyloid-like behavior in abiotic, amphiphilic foldamers, *J. Am. Chem. Soc.* 130 (2008) 1517–1524, doi:10.1021/ja0780840.
- [40] A. Hahma, S. Bhat, K. Leivo, J. Linnanto, M. Lahtinen, K. Rissanen, Pyrene derived functionalized low molecular weight organic gelators and gels, *New J. Chem.* 32 (2008) 1438–1448, doi:10.1039/B801708E.
- [41] J.-H. Ryu, E. Lee, Y. Lim, M. Lee, Carbohydrate-coated supramolecular structures: transformation of nanofibers into spherical micelles triggered by guest encapsulation, *J. Am. Chem. Soc.* 129 (2007) 4808–4814, doi:10.1021/ja070173p.
- [42] E. Lee, J.-K. Kim, M. Lee, Lateral association of cylindrical nanofibers into flat ribbons triggered by “molecular glue”, *Angew. Chem. Int. Ed.* 47 (2008) 6375–6378, doi:10.1002/anie.200801496.
- [43] Y. Liu, Y. Yu, J. Gao, Z. Wang, X. Zhang, Water-soluble supramolecular polymerization driven by multiple host-stabilized charge-transfer interactions, *Angew. Chem. Int. Ed.* 49 (2010) 6576–6579, doi:10.1002/anie.201002415.
- [44] S. Ghosh, S. Ramakrishnan, Small-molecule-induced folding of a synthetic polymer, *Angew. Chem. Int. Ed.* 44 (2005) 5441–5447, doi:10.1002/anie.200501448.
- [45] S. Ghosh, S. Ramakrishnan, Aromatic donor-acceptor charge-transfer and metal-ion-complexation-assisted folding of a synthetic polymer, *Angew. Chem. Int. Ed.* 43 (2004) 3264–3268, doi:10.1002/anie.200453860.
- [46] T. Haino, A. Watanabe, T. Hirao, T. Ikeda, Supramolecular polymerization triggered by molecular recognition between bisporphyrin and trinitrofluorenone, *Angew. Chem. Int. Ed.* 51 (2012) 1473–1476, doi:10.1002/anie.201107655.
- [47] J.-K. Kim, E. Lee, Z. Huang, M. Lee, Nanorings from the self-assembly of amphiphilic molecular dumbbells, *J. Am. Chem. Soc.* 128 (2006) 14022–14023, doi:10.1021/ja065487b.
- [48] E. Lee, Y.-H. Jeong, J.-K. Kim, M. Lee, Controlled self-assembly of asymmetric dumbbell-shaped rod amphiphiles: transition from toroids to planar nets, *Macromolecules* 40 (2007) 8355–8360, doi:10.1021/ma071511+.
- [49] Y. Kim, W. Li, S. Shin, M. Lee, Development of toroidal nanostructures by self-assembly: rational designs and applications, *Acc. Chem. Res.* 46 (2013) 2888–2897, doi:10.1021/ar400027c.
- [50] B. Shen, Y. Zhu, Y. Kim, X. Zhou, H. Sun, Z. Lu, M. Lee, Autonomous helical propagation of active toroids with mechanical action, *Nat. Commun.* 10 (2019) 1080, doi:10.1038/s41467-019-09099-9.
- [51] C. Tang, E.M. Lennon, G.H. Fredrickson, E.J. Kramer, C.J. Hawker, Evolution of block copolymer lithography to highly ordered square arrays, *Science* 322 (2008) 429–432, doi:10.1126/science.1162950.
- [52] H. Yan, S.H. Park, G. Finkelstein, J.H. Reif, T.H. LaBean, DNA-templated self-assembly of protein arrays and highly conductive nanowires, *Science* 301 (2003) 1882–1884, doi:10.1126/science.1089389.
- [53] M. Barboiu, G. Vaughan, R. Graff, J.-M. Lehn, Self-assembly, structure, and dynamic interconversion of metallosupramolecular architectures generated by Pb(II) binding-induced unfolding of a helical ligand, *J. Am. Chem. Soc.* 125 (2003) 10257–10265, doi:10.1021/ja0301929.